

morphologic characteristics of the cardiopulmonary system as an adaptation to chronic hypoxia (1), but there are few data concerning children living at high altitude. Standard 2-dimensional echocardiography was used to assess 477 healthy children (ages 15 days to 14 years; 220 Han living at 16-m altitude and 257 [117 Han and 140 Tibetans] at 3,700 m above sea level). Children in the 3,700-m group had lower arterial oxygen saturation ($p < 0.0001$), experienced slower increase in body weight and body surface area ($p = 0.04$ for both), and had a higher mean pulmonary arterial pressure (PA mean) ($p < 0.0001$). PA mean was 35.1 ± 8.9 mm Hg within 1 month of birth, rapidly decreased within 6 months (27.3 ± 11.8 mm Hg), and then gradually decreased to 23.3 ± 7.8 mm Hg at 14 years ($p = 0.003$). PA mean was maintained at about 15 mm hg in the 16-m group ($p = 0.09$). Dimensional increase in right atrium, right ventricle (RV), and RV outflow tract was faster with age ($p = 0.0008, 0.035,$ and <0.0001 , respectively). The main pulmonary artery was larger throughout the 14 years ($p = 0.04$), the decrease in RV mass was slower ($p = 0.005$), and RV ejection fraction was lower ($p < 0.0001$) (Table 1, Online Table 1).

Left heart morphology was not significantly different between the groups. Whereas left ventricular ejection fraction was not significantly different, left ventricular fractional shortening and the mean velocity of circumferential fiber shortening were lower ($p = 0.003$ for both). Interestingly, no significant difference was found in any variables between the Han and the Tibetan children living at 3,700 m (Table 1, Online Table 1).

Altitude adaptation implies a series of physiological changes to optimize oxygen supply. Pulmonary arterial hypertension is a consistent finding (2) that was observed in our study and its role in adaptation is less clear. Further supporting previous findings is the comparable left heart morphology to children living at sea level. Importantly, children at 3,700 m in our study showed distinctive adaptive features. First, the dilation of the right heart was predominant instead of hypertrophy. Second, there were subtle changes in diastolic and systolic function of both ventricles instead of the generally considered right-sided and diastolic dysfunction (2). Third, cardiac index was higher in children living at high altitude instead of being comparable to sea-level residents. Higher circulating concentrations of bioactive nitric oxide, leading to lower systemic vascular resistance with greater systemic blood flow to offset the hypoxemia, could be responsible (3). Some previous studies had suggested better high-altitude adaptation in people who were accustomed to live at high altitude for

centuries (e.g., Tibetans and natives of the Andes) compared with adaptation in low-altitude dwellers who migrate to and settle in high altitudes (e.g., the Han migrating to Tibet in the last 50 years). In our study, it was interesting that both Han and Tibetan children had comparable cardiopulmonary adaptive responses at high altitude.

Hai-Ying Qi, MD
Ru-Yan Ma, MD
Li-Xia Jiang, MD
Shu-Ping Li, MD
Shu Mai, MD
Hong Chen, MD
Mei Ge, MD
Mei-Ying Wang, MD
Hai-Ning Liu, MD
Yue-Hong Cai, MS
Su-Ya Xu, MD
Jia Li, MD, PhD*

*Clinical Physiology Research Center
Capital Institute of Pediatrics
2 Yabao Road
Beijing, 100020
China

E-mail: jt11@yahoo.com

<http://dx.doi.org/10.1016/j.jcmg.2014.04.027>

Please note: This study was funded by institutional funds. The authors have reported that they have no relationships relevant to the contents of this paper to disclose.

REFERENCES

1. Penalzoza D, Arias-Stella J. The heart and pulmonary circulation at high altitudes: healthy highlanders and chronic mountain sickness. *Circulation* 2007;115:1132-46.
2. Sime F, Banchemo N, Penalzoza D, Gamboa R, Cruz J, Marticorena E. Pulmonary hypertension in children born and living at high altitudes. *Am J Cardiol* 1963;11:143-9.
3. Erzurum SC, Ghosh S, Janocha AJ, et al. Higher blood flow and circulating NO products offset high-altitude hypoxia among Tibetans. *Proc Natl Acad Sci U S A* 2007;104:17593-8.

APPENDIX For a supplemental table, please see the online version of this paper.

3D Image Reconstruction of Histopathological Structure of Atherosclerotic Plaque Using a Novel Technique With Film Tomography



Pathology studies of atherosclerosis have contributed much to our understanding, but they are based mainly on cross-sectional views of the postmortem artery samples. Atherosclerosis is, however, a dynamic 3-dimensional (3D) pathological process and 3D imaging techniques such as intravascular ultrasound

or optical coherence tomography are in vogue. However, these techniques still have limitations in defining histological structure of the plaque, and advances in histology techniques might enhance the contribution of pathological studies.

Mitsumori et al. (1), have developed a technique called “film tomography” to prepare tissue sections with an adhesive film. An automatic microtome can consecutively cut the paraffin-embedded tissue blocks into 6- μm -thick sections (approximately 1,600 slides from a 1-cm long tissue sample) and then put the sections on a long film roll in a row. The sections-on-film are automatically placed in a plastic frame that

can be processed with usual pathological or immunohistochemical stains.

This is the first report of applying this technique to 3D assessment of atherosclerosis of postmortem human coronary arteries. Consecutive slides could be reconstructed as a longitudinal section, an exterior imaging of the whole vessel body, a translucent whole vessel imaging for depiction of tissue distribution, a walk-through or fly-through movie, or color enhancement processing for identifying specific tissue within the stained vessel. These 3D images can be moved, rotated, shifted, or cross sectionally sliced arbitrarily on the computer. Representative static

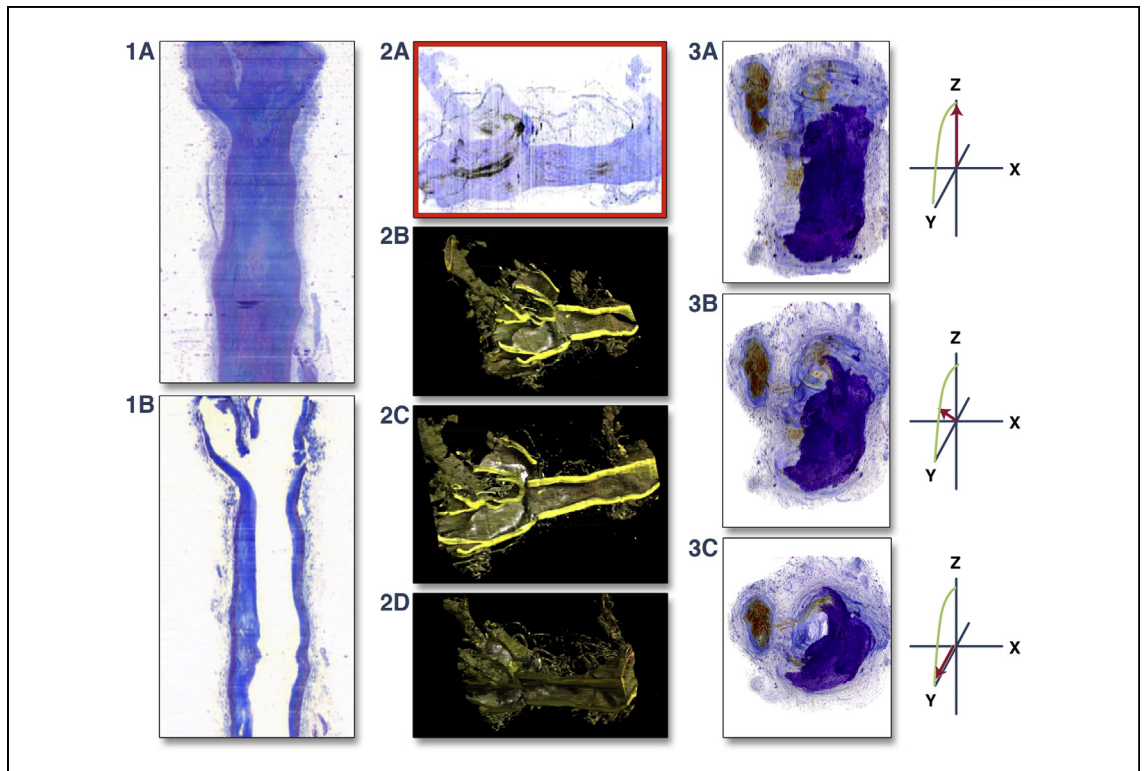


FIGURE 1 Representative 3D Histopathological Images of Coronary Atherosclerotic Plaque With Film Tomography

A representative 3-dimensional (3D) translucent whole body imaging of coronary arterial segment (1A) and its reconstructed longitudinal cross-sectional image (1B) with Masson trichrome stain are shown. As with the regular trichrome stain, the **red** color corresponds to smooth muscle, the **blue** to fibrous tissue, and the **white** to lipidic tissue. The stereoscopic or longitudinal distribution of these components can be readily identified. Representative reconstructed images of the longitudinal section of a coronary arterial segment with the original CD68 stain (2A) and its stereoscopic 3D images (2B to 2D) are demonstrated. In the original stain (2A), the **dark brown** area corresponds to macrophage accumulation. 2B to 2D, which are longitudinal half-cuts of the vessel whole body from 3 different view angles, were made from computer-derived color processing in order to clearly visualize macrophage accumulation and vessel wall border. In 2B to 2D, the **white** area corresponds to macrophage accumulation. Representative images of 3D color-processed translucent whole body imaging with a composite of hematoxylin and CD68 stain from 3 different angles within the same rotation circle are provided from a coronary segment (3A to 3C). The angles of the longitudinal axis of the imaged vessel in the x-y-z coordinate are denoted by the **red arrow** in the right side of each panel for reference. In 3A to 3C, **purple** corresponds to calcified area and **brown** to macrophage accumulation. Macrophages can be seen around the branch of this vessel. It is noteworthy that this system does not tear the vessel at all during the histological processing, and that we are able to clearly overview the stereoscopic distribution of calcification, even when there is a significant calcified mass within the vessel.

images of the coronary artery with use of this technology are shown in **Figure 1**. These capabilities of the 3D film tomography would give a new insight into atherosclerosis and could provide a new comparative standard for intravascular imaging with a 3D reconstruction.

Takafumi Hiro, MD, PhD*
Tadateru Takayama, MD, PhD
Hironori Haruta, MD, PhD
Masayuki Mitsumori, PhD
Kimio Tanaka, PhD
Junichi Kawanabe, PhD
Sumihare Noji, PhD
Atsushi Hirayama, MD, PhD

*Division of Cardiology
Department of Medicine
Nihon University School of Medicine
30-1 Oyaguchi-kamicho
Itabashi-ku, Tokyo 173-8610
Japan
E-mail: hiro.takafumi@nihon-u.ac.jp
<http://dx.doi.org/10.1016/j.jcmg.2014.04.028>

REFERENCE

1. Mitsumori M, Adachi T, Takayanagi K, et al. Film tomography as a tool for three-dimensional image construction and gene expression studies. *Dev Growth Differ* 2007;49:583-9.

Tricuspid Regurgitation Severity Associated With Positioning of RV Lead or Other Etiology Assessed by Intracardiac Echocardiography



We read with interest the report by Mediratta et al. (1), which concluded that an intercommissural or middle-of-the-annulus position is desired to minimize device-related tricuspid regurgitation (TR) post-implantation of right ventricle (RV) pacemaker and implantable cardioverter-defibrillator (ICD) leads. In their methodology, the RV lead location is determined by 3-dimensional (3D) transthoracic echocardiography (TTE) and the severity of TR, only by 2-dimensional (2D) color Doppler evaluation. Finally, they suggested that 3D TTE should be routinely used during intraprocedural lead placement. Several important issues, especially factors related to assessment of the severity of TR in this retrospective study, need to be clarified.

Although not considered by Mediratta et al. (1), causes of TR other than lead placement may be critical. TR may be due to either intrinsic valvular disease/dysfunction (leaflet, chord, or papillary muscle) or tricuspid annulus enlargement. For patients with

cardiac devices, the most frequent change in RV morphology is dilation due to chronic elevation of left heart filling pressures and subsequent development of pulmonary hypertension. When pulmonary artery systolic pressure (PASP) exceeds 40 mm Hg, the incidence of TR approaches 90% (2). Due to lack of focus during retrospective analysis on etiological factors and time interval dependence between device implantation and 3D TTE study, one could question whether TR is caused by underlying heart disease or lead location. In their Figures 1 and 4 (1), moderate-to-severe RV dysfunction was apparent in an example of septal impingement by a device lead, whereas a normal/smaller RV chamber was shown in their example (Figure 5) (1) of a well-positioned lead. There must be other factors involved; otherwise, what would explain the greater baseline severity of TR in the lead impingement group as shown in their Figure 6 (1)? Paired comparison data for the subgroup patients with 2D TTE before and after implantation (n = 53) should have been shown separately.

With routine clinical application of intracardiac echocardiography (ICE), RV anatomy and function (3) and many of the valvular etiologies of TR can be identified and assessed in real time. Real-time ICE imaging has superior capability to image the course of the device lead from the right atrium to the RV. The device-lead location and route passing through the annulus can be imaged. TR induced by intracardiac device-lead impingement and its severity can be accurately assessed (Figures 1A and 1B). However, independent of lead position, moderate-to-severe and mainly centralized TR can be commonly detected in an enlarged and dysfunctional RV, secondary to left ventricular (LV) dysfunction/heart failure (Figures 1C and 1D) or due to arrhythmogenic RV cardiomyopathy (Figures 1E and 1F) with recurrent ventricular tachyarrhythmia. It is strange that this paper found no difference in TR severity in ICD versus pacemaker lead implantation. Our clinical observations with ICE imaging may indicate that ICD leads with more thickness and rigidity have higher events of TR than standard pacing leads, as others have reported previously (4).

Iatrogenic lead-related TR is an important clinical problem, and the investigators should be congratulated for reporting a relatively large number of cases with 2D and 3D TTE imaging. However, their results do not consider other important causes for TR and certainly did not demonstrate convincingly how real-time 3D TTE would consistently facilitate lead placement.